Report No.: SIR-97-029
Revision No.: 0
Project No.: DECO-01Q
Project File No.: DECO-01Q-401
March 1997

Leak-Before-Break Evaluation for Three Locations on the Recirculation System at Fermi 2

Prepared for:

Detroit Edison Company

Prepared by:

Structural Integrity Associates, Inc.
San Jose, CA

Prepared by: _____ Date: 3/25/97
G. A. Miessi

_____ Date: 3/25/97
P. L. Chen

_____ Date: 3/25/97
N. G. Cofie

Reviewed and Approved by: _____ Date: 3/25/97
P. C. Riccardella

9704080264 970404
PDR ADOCK 05000341
P PDR

REVISION CONTROL SHEET

Document Number: SIR-97-029

Title: Leak-Before-Break Evaluation for Three Locations on the Recirculation System at Fermi 2

Client: Detroit Edison Company

SI project Number: DECO-010

Section	Pages	Revision	Date	Comments
i-v	all	0	3/25/97	Initial Issue
1	1-1 to 1-4	0	3/25/97	Initial Issue
2	2-1 to 2-2	0	3/25/97	Initial Issue
3	3-1 to 3-2	0	3/25/97	Initial Issue
4	4-1 to 4-6	0	3/25/97	Initial Issue
5	5-1 to 5-20	0	3/25/97	Initial Issue
6	6-1	0	3/25/97	Initial Issue
7	7-1 to 7-2	0	3/25/97	Initial Issue
Appendix A	A-0 to A-10	0	3/25/97	Initial Issue

EXECUTIVE SUMMARY

This report documents evaluations performed by Structural Integrity Associates to determine the leak-before-break (LBB) capabilities at three locations on the recirculation system piping at Fermi 2. The three locations are adjacent to the reactor pressure vessel on two 12-inch discharge risers and one 28-inch suction line. At each of these locations, three closely spaced welds; nozzle-to-safe end (N-SE), safe end-to-pipe (SE-P) and pipe-to-elbow (P-E) were considered as potential break locations.

The evaluations were performed taking guidance from NUREG-1061, Vol. 3 which provides NRC accepted methodology and criteria for performing LBB analysis. Additional guidance was taken from EPRI Report NP-4991 which provides specific application of LBB to BWR piping. In summary, the LBB methodology involves the determination of through-wall critical flaw size (unstable throughwall flaw length) for the piping system component under normal plus SSE seismic loads and then computing the leakage under normal loads through a fraction of the critical flaw size (leakage flaw size). NUREG-1061. Vol. 3 requires a safety factor of two between the critical flaw size and the leakage flaw size. The computed leakage is then compared to the plant detection system to ensure that the leakage through the leakage flaw can be detected. Circumferential flaws are considered since they are more limiting than axial flaws.

Critical flaw sizes were calculated using elastic-plastic fracture mechanics and lower bound material properties for the components. The calculated critical flaw sizes for the 12-inch risers ranged from 6.71 inches to 13.82 inches. The critical flaw sizes for the 28-inch suction line range from 24.53 inches to 27.97 inches.

Leakage was calculated for throughwall flaws of various fractions of the critical flaw size. For the 12-inch risers the minimum leakage at one-quarter critical flaw size is about 0.2 gpm. The leakage increases to approximately 1.5 and 5 gpm at one-half and three-quarters the critical flaw size, respectively. The corresponding leakages for the 28-inch suction line are about 1.5, 10 and 35 gpm respectively.

Even though the IGSCC resistance of all the welds considered in this evaluation have been treated by NUREG-0313, Revision 2 accepted IGSCC improvement processes, a conservative IGSCC evaluation was performed using the NUREG-0313, Revision 2 bounding crack growth law to determine times to grow from various sub-critical flaw sizes to the critical flaw sizes. The evaluation showed that it takes at least one cycle (over eighteen months) for a through-wall crack at half the critical flaw size to grow to three quarters the critical flaw size. This demonstrates that there is adequate time for the plant to take appropriate action before the critical flaw size is reached, once the leakage rates determined in this report are detected by the plant monitoring systems.

The effect of degradation mechanisms which could impact the LBB evaluations were considered in the evaluation and it was concluded that they would have no effect on the results. These mechanisms are water hammer, corrosion (intergranular stress corrosion cracking (IGSCC) and erosion-corrosion) and fatigue. Experience from the BWR industry has shown that water hammer is not a concern for the recirculation system. All welds considered in this evaluation are resistant to IGSCC based on the fact that they have received mechanical stress improvement process (MSIP), induction heating stress improvement (IHSI) or were solution annealed. The material of the recirculation system is Type 304 stainless steel which is not susceptible to erosion-corrosion. Since severe thermal transients and other cyclic loads are not expected in the recirculation system, there is no active mechanism to lead to fatigue crack growth.

Table of Contents

List of Tables

List of Figures

1.0 INTRODUCTION

1.1 Background

This report documents evaluations performed by Structural Integrity Associates (SI) to determine the leak-before-break capabilities at three locations on the recirculation system at Fermi 2. These evaluations are necessary because a pipe break at these locations could impact the safety function of the Emergency Equipment Cooling Water (EECW) system which is in the vicinity of these postulated break locations.

The three locations considered in this evaluation are shown in Figure 1-1[11]. All three locations are in close proximity of reactor pressure vessel nozzles. The first location is on 12-inch discharge riser N2F in the "A" loop. The second and third locations are on 12-inch discharge riser N2D and 28-inch section line N1B. on the "B" loop. At each of these locations, there are three closely spaced welds as shown in Figure 1-2; nozzle-to-safe end (N-SE), safe end-to-pipe (SE-P) and pipe-to-elbow (P-E). All these welds are considered as potential break locations in this evaluation.

1.2 Leak-Before-Break Methodology

The concept of leak-before-break (LBB) implies that any crack or defect which develops in a component will grow to a through-wall configuration, and thus be detected by plant monitoring systems before reaching a size that would significantly reduce margins to component rupture in the plant. NUREG-1061, Vol. 3 [1] provides the methodology and criteria for application of LBB for the elimination of protective structures such as pipe whip restraints, jet impingement shields etc., which provide protection against pipe break. In the context used in this evaluation, LBB is part of an overall assessment to determine suitability for continued plant operation with respect to the safety function of the EECW system, assuming postulated through-wall flaws, using the criteria outlined in NUREG-1061, Vol. 3. Additional guidance on the application of LBB specifically to BWR piping is provided in Ref. 2. In summary, the approach provided in NUREG-1061, Vol. 3 approach involves the determination of through-wall critical flaw size for the piping system component under normal

plus SSE seismic loads and then computing leakage under only normal loads through a flaw with a length equal to one half of the critical flaw size (the leakage flaw size). The computed leakage is then compared to the plant detection systems to ensure that the leakage through this flaw can be detected. The acceptance criteria for LBB evaluation per NUREG-1061, Vol. 3 [1] are provided in Section 2 of this report. The applicable criteria will be used for the LBB evaluation for the three break locations on the recirculation system at Fermi 2.

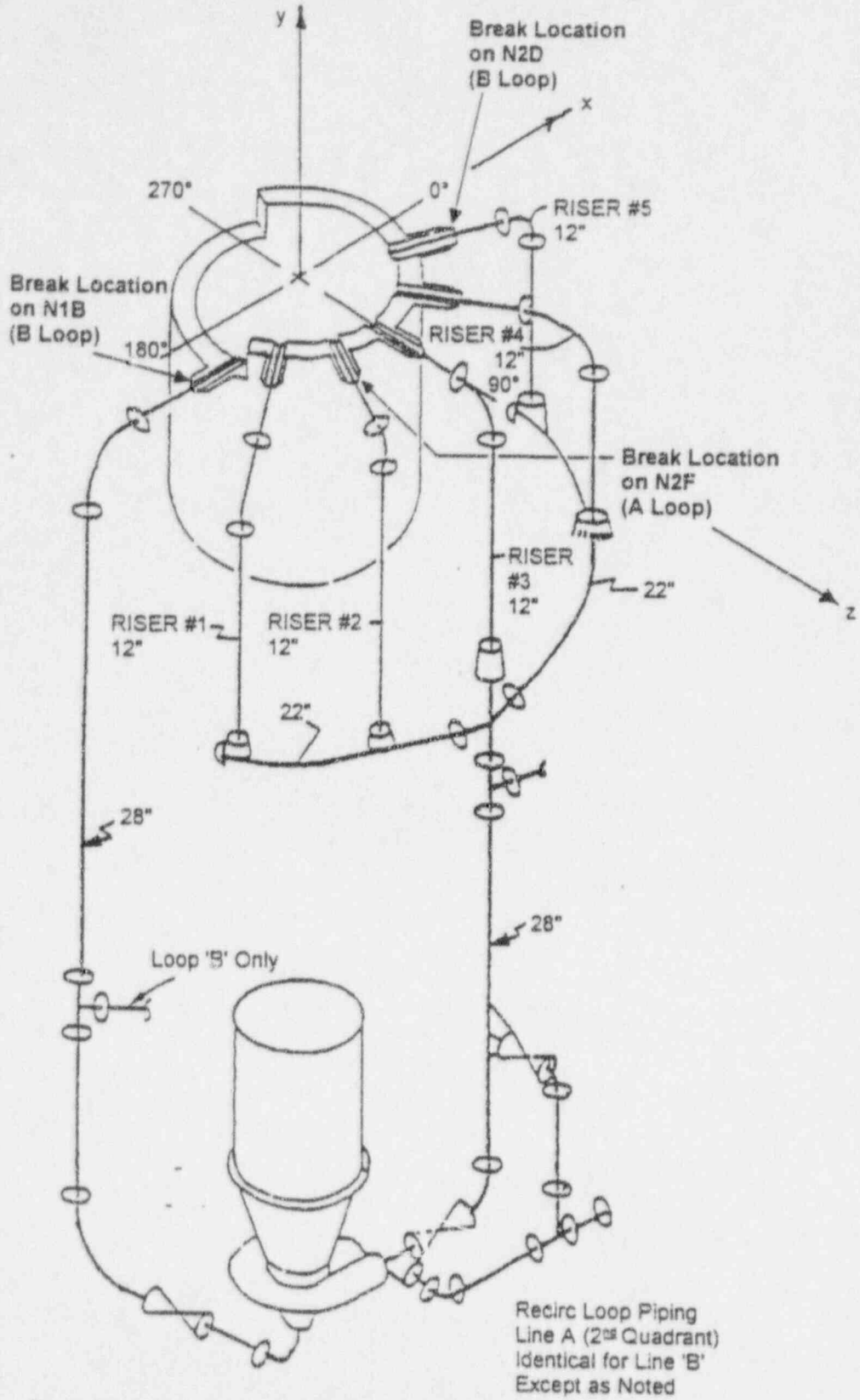

Figure 1-1. Postulated Break Locations for the LBB Evaluations in the Recirculation System Loops A and B at Fermi 2

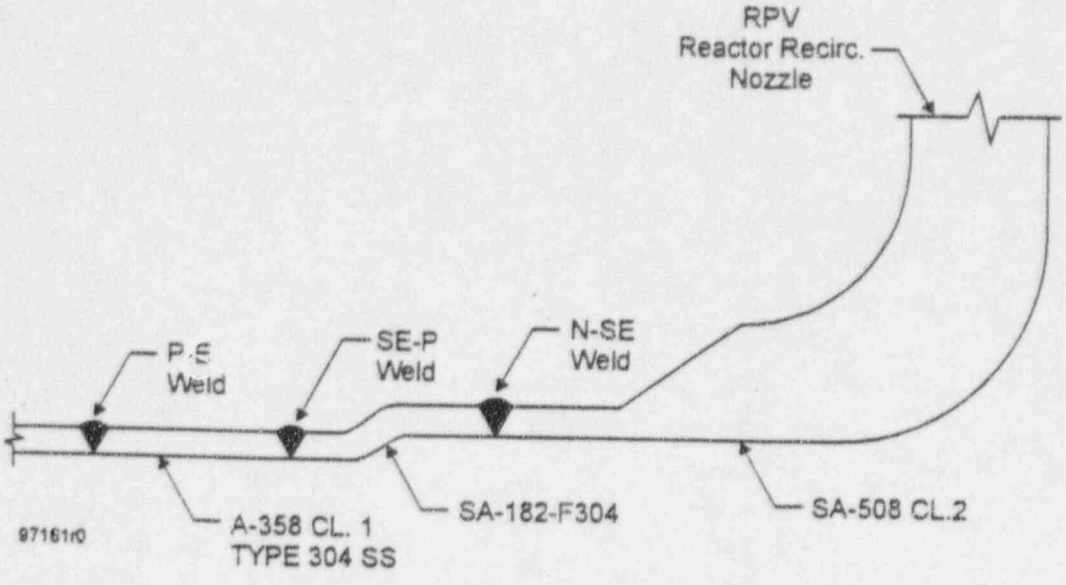

Figure 1-2. Details of Weld Configurations at the Locations for LBB Evaluations

2.0 CRITERIA FOR APPLICATION OF LEAK-BEFORE-BREAK APPROACH

NUREG-1061, Volume 3 [1] identifies several criteria to be considered in determining applicability of the leak-before-break approach to piping systems.

Section 5.2 of Reference 1 provides an extensive discussion of the criteria for performing leak-before-break analyses. The details of that discussion will not be repeated here, but a summary of the various requirements as applied to the three locations on the recirculation system at Fermi 2, is provided.

2.1 Criteria for Through-Wall Flaws

Acceptance criteria for critical stresses and critical flaws are:

1. The flaw size that is required to produce an "acceptable leakage rate" shall be smaller than the critical flaw length associated with the maximum stress, including safe shutdown earthquake (SSE) seismic loadings, by a factor of 2.

2. The stress required to make the "acceptable leakage rate" flaw critical shall be greater than the maximum stress (with SSE) by a factor of at least $\sqrt{2}$.

3. The net section collapse criterion (NSCC) evaluation approach may be used to compute the critical flaw size provided a safety factor of 3 is placed on the combination of normal operation plus safe shutdown earthquake stresses.

It has been found in previous LBB evaluations conducted by Structural Integrity Associates (SI), that the second and third criteria stated above are generally not bounding. The method described in the first criteria provides a smaller leakage rate than the second criteria. Therefore, only the first criteria will be considered in this report. Furthermore, elastic-plastic fracture mechanics (EPFM) approach is generally conservative relative to the NSCC approach when applied to stainless steel piping. Therefore, only EPFM principles will be applied in this evaluation.

2.2 Criteria for Part-Through-Wall Flaws

NUREG-1061 requires demonstration that a long part-through-wall flaw which is detectable by ultrasonic means will not grow due to fatigue to a depth which would produce instability over the life of the plant. Previous studies performed by Structural Integrity (SI) have shown that in all cases, fatigue crack growth is not very significant and does not affect the outcome of the LBB studies especially for the recirculation system of a BWR in which there is little cyclic loading. Hence, in this evaluation, fatigue crack growth evaluation will not be performed.

2.3 Other Mechanisms

NUREG-1061 limits applicability of the leak-before-break approach to those locations where degradation or failure by mechanisms such as water hammer, erosion/corrosion, and intergranular stress corrosion cracking (IGSCC) is not a significant possibility. These mechanisms were considered for the locations under evaluation and are discussed in Section 3 of this report.

3.0 CONSIDERATION OF WATER HAMMER, CORROSION AND FATIGUE

NUREG-1061, Volume 3 [1] states that LBB should not be applied to high energy lines susceptible to failure from the effect of water hammer, corrosion or fatigue. These potential failure mechanisms are thus discussed below with regard to the recirculation system at Fermi 2. It is concluded that the above failure mechanisms do not invalidate the use of LBB for the affected locations on the recirculation system at Fermi 2.

3.1 Water Hammer

Several studies performed on water hammer experience in the industry have indicated that the recirculation system of a BWR is not susceptible to water hammer events. A very comprehensive discussion of the industry experience is provided in NUREG-1061, Vol. 4 [3] and NUREG-0927 [4]. Section 4.2 of Reference 2 provides specific evaluation of water hammer potential in the recirculation system of a BWR and concludes that water hammer is not a significant event for this system.

3.2 Corrosion

Two corrosion damage mechanisms which can lead to rapid piping failure are intergranular stress corrosion cracking (IGSCC) in austenitic stainless steel pipes and flow-assisted corrosion (erosion-corrosion or cavitation, primarily) in carbon steel pipes. Although the Type 304 stainless steel piping material for the recirculation system at Fermi 2 is susceptible to IGSCC, the following processes have been applied to the weldments shown in Figure 1-2 to make them resistant to IGSCC.

- The nozzle-to-safe end welds received mechanical stress improvement process (MSIP)
- The safe end to pipe welds received induction heating stress improvement (IHSI) treatment
- The pipe to elbow welds were connected in the shop and solution annealed after welding

All these processes are considered acceptable means by NUREG-0313, Revision 2 [5] for mitigating these welds against IGSCC.

Erosion-corrosion is a mechanism limited to carbon steel piping. It is not a problem for stainless steel pipes and components. Cavitation damage occurs only at valves used for flow control. As such, neither of these mechanisms is anticipated to be an active degradation mechanism for the recirculation system at Fermi 2.

3.3 Fatigue

As mentioned in Section 2.2 of this report, fatigue analyses will not be performed in this report since previous studies performed by SI have shown that fatigue crack growth is generally insignificant. Since severe thermal transients and other cyclic loads are not expected in the recirculation system, there is no active mechanism to lead to fatigue crack growth.

4.0 PIPING MATERIALS AND STRESSES

4.1 Material Properties

The piping materials at the locations considered in the LBB evaluation are shown in Figure 1-2. The pipe and safe end materials are Type 304 stainless steel. The safe end is welded to the SA 508 Class 2 nozzle using Inconel 182 weld metal. Per the welding specification which was used for fabrication, several processes were used for the welding including submerged arc welding (SAW), shielded metal arc welding (SMAW), gas tungsten are welding (GTAW) and gas metal arc welding (GMAW). Weldments resulting from the non-flux processes (GTAW and GMAW) have been shown to exhibit very high toughness and therefore have superior flaw tolerance. These materials typically fail by net section plastic collapse (limit load) [6]. However, the flux weldments (SAW and SMAW) have relatively low ductility and toughness. As such, they exhibit unstable crack extension before the flawed pipe section reaches the limit load associated with the non-flux weld flow stresses [6]. In order to perform a bounding evaluation, the flux weldment properties will be used in this report.

The material properties used in the elastic-plastic fracture mechanics analyses are shown in Table 4-1, and represent lower bound flux weldment toughness properties published in the literature [6, 7]. The elastic modulus (E), Code allowable stress intensity (Sm), and lower bound yield strength ($\sigma_o=\sigma_y$) and ultimate strength (σ_u) were taken from Section III of the ASME Boiler & Pressure Vessel Code [8] for the temperatures of interest. The flow stress is computed as an average of σ_y and σ_u, although this does not influence the stability analysis results. Ramberg-Osgood true stress-strain parameters, α and n, and the J-resistance material properties, are taken from Reference 7. Plots of the stress-strain curve and the J-resistance curve are shown in Figures 4-1 and 4-2, respectively.

4.2 Piping Stresses

The piping stresses which are normally considered in a LBB evaluation are due to normal operating condition (NOC) which includes pressure, deadweight and thermal expansion while the reactor is at full power combined with Safe Shutdown Earthquake (SSE). The piping loads for the various weld locations were obtained from Reference 9 and are presented in Appendix A. Geometric data for calculating the stresses was obtained from Reference 10. Stresses for LBB evaluation were conservatively calculated considering the torsional moment. For calculation of critical flaw size, the stress combination due to NOC and SSE loads is used. For leakage calculations, the stress combination due to NOC is used. These stress combinations are shown in Tables 4-2.

The axial stress due to internal pressure is calculated from the expression:

$$\sigma_{axial} = \frac{pR_i^2}{(R_o^2 - R_i^2)}$$

where p is the internal pressure, R_o is the outside radius, and R_i is the inside radius. A pressure of 1047 psig was used for the suction side while 1254 psig was used for the discharge piping [11].

The dead weight and thermal stresses were calculated from the relationship:

$$\sigma = \frac{F_a}{A} + \frac{M}{Z}$$

where:

F_a is axial force

M is the resultant moment = $\sqrt{M_a^2 + M_b^2 + M_c^2}$

M_a is the torsional moment

M_b, M_b, are the bending moments in b and c directions, respectively.

A is pipe cross-sectional area

Z is the section modulus.

A summary of the stresses calculated from these loads for the various welds is presented in Table 4-2, which also shows the stress combinations for calculation of critical flaw size as well as the stress combinations for determination of leakage.

Table 4-1

Material Properties Used for Type 304 Stainless Steel in LBB Evaluation

E (ksi)	25,570
σ_o (ksi) ($= \sigma_y$)	18.85
σ_u (ksi)	63.0
σ_{flow} (ksi)	41.18
α	11.56
n	2.88
J_{Ic}(in-kip/in^2)	0.30
J_{max} (in-kip/in^2)	5.0
C	2.673
N	0.3162

Table 4-2

Summary of Stresses

Location	Weld	STRESS (ksi)					
		PRESSURE	DEAD WT.	THERMAL	S.S.E.	P+DW+TH	P+DW+TH+SSE
Loop A N2F	N-SE	2.883	0.339	3.104	2.587	6.326	8.913
	SE-P	4.694	0.512	5.055	4.393	10.261	14.654
	P-E	4.694	0.173	2.909	3.895	7.776	11.671
Loop B N2D	N-SE	2.883	0.359	2.440	3.042	5.682	8.724
	SE-P	4.694	0.531	4.012	4.790	9.236	14.026
	P-E	4.694	0.136	2.065	2.578	6.894	9.472
Loop B N1B	N-SE	3.548	0.102	1.354	2.356	5.004	7.360
	SE-P	3.994	0.117	1.578	2.430	5.689	8.119
	P-E	3.994	0.106	1.757	1.366	5.856	7.223

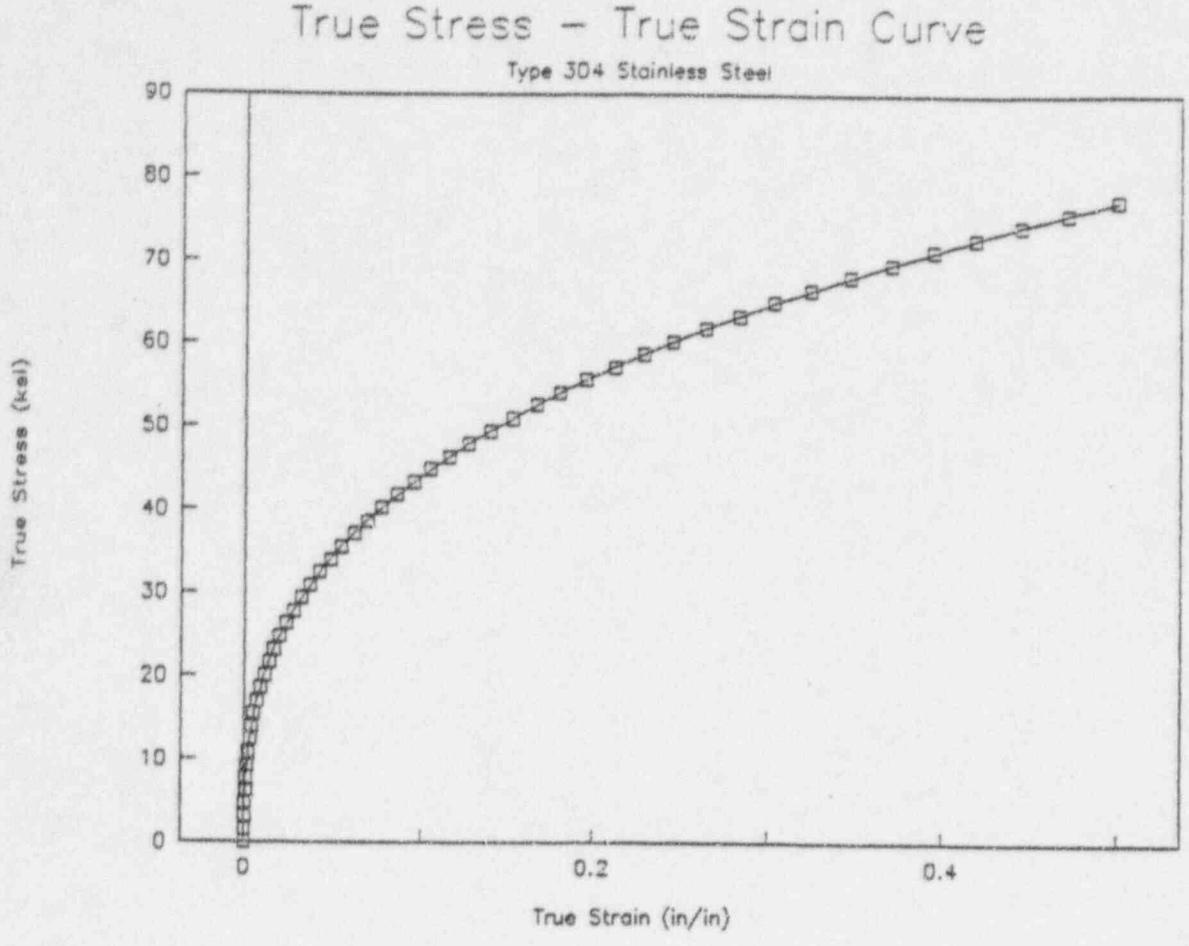

Figure 4-1. Ramberg-Osgood True Stress-True Strain Curve for Type 304 Stainless Steel

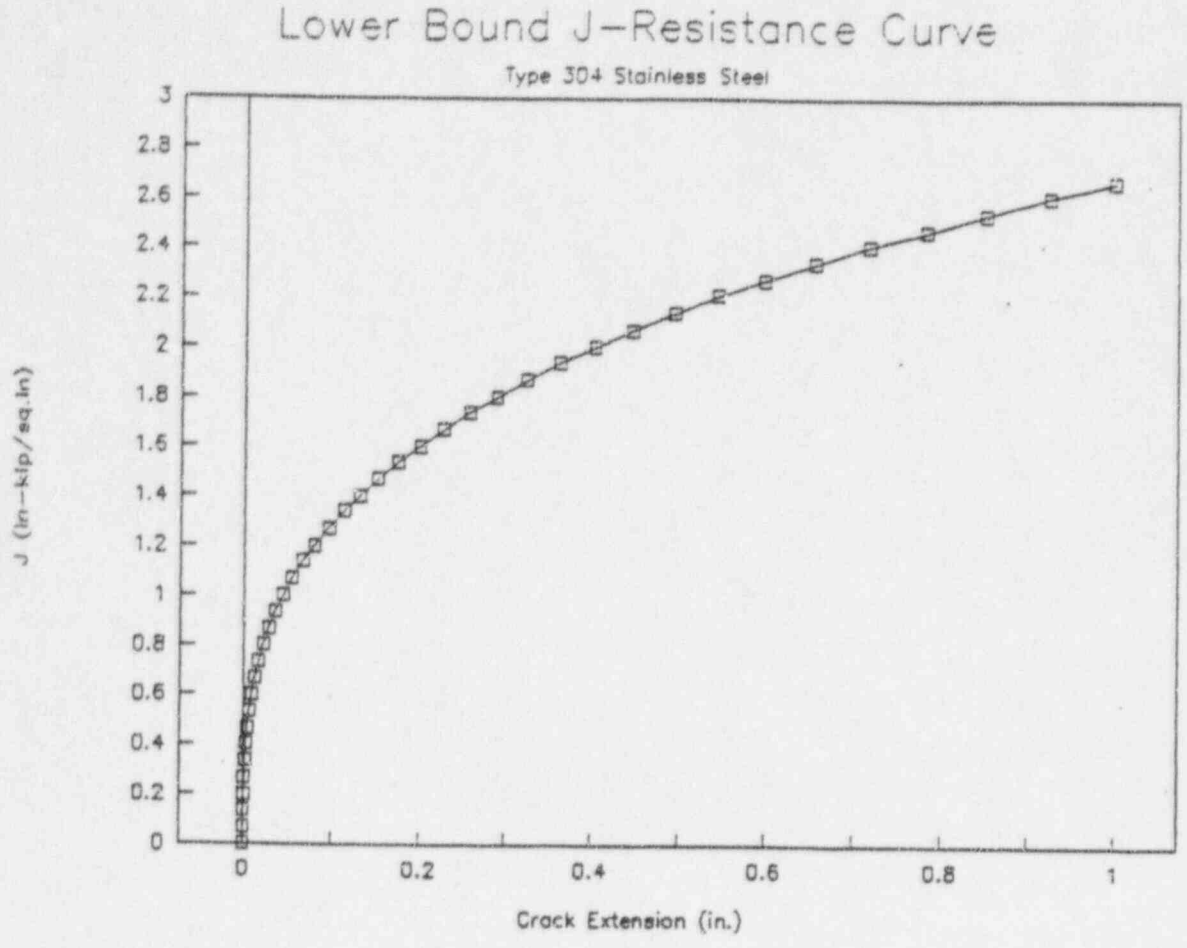

Figure 4-2. Lower Bound J-Resistance Curve for Type 304 Stainless Steel

5.0 LEAK-BEFORE-BREAK EVALUATION

The LBB approach involves the determination of critical flaw sizes, critical stresses and leakage through postulated flaws. The critical flaw length for a through-wall flaw is that length for which, under a given set of applied stresses, the flaw would become marginally unstable. Similarly, the critical stress is that stress at which a given flaw size becomes marginally unstable. NUREG-1061, Volume 3 [1] defines required margins of safety on both flaw length and applied stress. However, as explained in Section 2, safety margins based on flaw length have been found in previous evaluations to be the more conservative of the two and therefore, only the criterion based on flaw length will be used in this evaluation. Furthermore, previous evaluations have demonstrated that circumferential flaws are more restrictive than postulated axial flaws. For this reason, the evaluation presented herein will concentrate on circumferential flaws.

5.1 Evaluation of Critical Flaw Sizes

Critical flaw sizes may be determined using the net section collapse criterion (NSCC) approach or the J-Integral/Tearing Modulus (J/T) methodology. NSCC is particularly suited for materials with extreme amounts of ductility and toughness such as wrought stainless steel materials, since it assumes that the cross section of the pipe becomes fully plastified at the onset of failure. For materials with lower toughness, J/T methodology is used. In this evaluation, the critical flaw sizes will be determined based on the J/T approach.

Methods for calculations of J and T for the stability assessment of through-wall circumferential flaws in cylindrical geometries such as pipes has been developed by EPRI in References 12, 13, and 14. This methodology was used for the determination of critical flaw sizes using the Structural Integrity Associates computer program, **pc-CRACK** [15].

The expression for the J-integral for a through-wall circumferential crack under tension loading [12] which is applied in this analysis is:

$$J = f_1\left(a_e, \frac{R}{t}\right)\frac{P^2}{E} + \alpha\,\sigma_o\,\varepsilon_o\,c\left(\frac{a}{b}\right)h_1\left(\frac{a}{b}, n, \frac{R}{t}\right)\left[\frac{P}{P_o}\right]^{n+1}$$

where

$$f_1\left(a_e, \frac{R}{t}\right) = \frac{a_e F^2\left(\frac{a}{b}, \frac{R}{t}\right)}{4\pi R^2 t^2}$$

a_e = effective crack length including small scale yielding correction

R = nominal pipe radius

t = pipe wall thickness

F = elasticity factor

P = applied load = $\sigma_\infty \cdot 2\pi Rt$; where σ_∞ is the remote tension stress in the uncracked section

α = Ramberg-Osgood material coefficient

E = elastic modulus

σ_o = yield stress

ε_o = yield strain

c = b-a

$2a$ = crack length

$2b$ = $2\pi R$

h_1 = plasticity factor

P_o = limit load corresponding to a perfectly plastic material

n = Ramberg-Osgood strain hardening exponent.

Similar equations [12,13,14] are used to compute critical flaw sizes for circumferential through-wall cracks under bending stresses. Crack extensions during stable ductile tearing in the EPFM analyses are conservatively subtracted from the critical flaw length computations.

The piping stresses consist of tension, bending and torsion stresses. The tension stress is due to internal pressure while the bending and torsion stresses are caused by deadweight, thermal and seismic loadings. As described above, only the pure tension or pure moment models were determined to be applicable. Thus, fracture mechanics solutions were developed for two cases: 1) the total axial stress was considered to be tension and 2) the total axial stress was considered to be bending. Then, the critical flaw sizes obtained with the tension model (a_t) and with the bending model (a_b) were combined to determine the actual critical flaw size (a_c) due to combined tension and bending stress. Linear interpolation was used as described by the following equation:

$$a_c = a_t \left(\frac{\sigma_t}{\sigma_b + \sigma_t} \right) + a_b \left(\frac{\sigma_b}{\sigma_b + \sigma_t} \right)$$

This approach has been shown to provide a good representation of the critical flaw size for combined state of stress. Clearly, it provides the exact answer at the extremes of pure tension and pure bending.

For calculation of critical flaw sizes, the worst loading condition associated with using the resultant bending moment (including torsion effects) have been included. This is conservative and will result in the smallest possible critical flaw size. The critical flaw sizes are shown in Table 5-1.

5.2 Leak Rate Determination

The determination of leak rate is performed using the Structural Integrity Associates proprietary program, **pc-LEAK** [16]. The methodology employed in **pc-LEAK** involves the determination of crack opening area (COA), with consideration of local plasticity at the crack tip. Then, the flow rate is determined based on classical thermal-hydraulic expressions for single and two-phase flow.

Crack opening area under the influence of steady-state operating stress (combined tension and bending) is computed from References 17 and 18 as:

$$A_e = \frac{\sigma_t}{E} (\pi R^2) I_t (\theta) \left[1 + \frac{\sigma_b}{\sigma_t} \left(\frac{3+\cos\theta}{4} \right) \right]$$

where:

A_e = crack opening area (in^2) including plastic zone correction, assuming plane stress

σ_t = steady-state tension stress (psi)

σ_b = steady-state axial bending stress (psi)

E = elastic modulus (psi)

R = nominal pipe radius (in.), and

θ = the angle describing half the through-wall crack length (radians).

The term $I_t(\theta)$ is computed for varying R/t (pipe radius/thickness) in accordance with the equations of Reference 17.

The plastic zone correction for the effect of yielding near the crack tip is incorporated by the following equation [17]:

$$\theta_e = \theta + \frac{K_{total}^2}{2\pi R \sigma_o^2}$$

where:

θ_e = effective half-length of angle through-wall crack, assuming plane stress

K_{total} = stress intensity factor due to combined tension and bending

σ_o = material reference stress (flow stress = ½ (σ_y + σ_u) was used in this study, where σ_u = ultimate tensile strength

σ_y = yield strength (0.2%)

The flow rate through the crack is based on classical thermal-hydraulic methodology. The development of the approach is detailed in the following section. The methodology includes considerations of both liquid and vapor flow of water, including the consideration of two phase flow within the crack.

The crack is considered to have a total length of 2a either around the circumference or axially along the pipe wall. The crack has an average opening width w, and the flow path length through the wall is taken as L.

The hydraulic diameter [19] of the flow path is:

$$D_H = \frac{4A}{P}$$

where:

D_H = hydraulic diameter

A = cross-sectional area

P = perimeter

For a narrow crack of length 2a,

$$D_H = \frac{4 \times A}{(2)\ (2a)} = \frac{A}{a}$$

If w is the average crack opening width, then

$$A = 2aw$$

and

$$D_H = 2w$$

The frictional loss in the constant area channel will be assumed to be that between parallel plates with a surface roughness. The parameter of interest to characterize the flow resistance per unit of area is:

$$K_{eff} + K_{exit} = \Sigma K_i + \frac{fL}{D_H} + K_{exit}$$

where:

K_{eff} = effective total pressure loss coefficient

K_i = individual discontinuity total pressure loss coefficient

f = friction factor

L = flow path length, (pipe wall thickness)

D_H = hydraulic diameter

K_{exit} = exit loss coefficient = 1.0

The pressure loss coefficients for the entrance and flow direction changes must be computed separately from the friction loss parameters. For example, Reterence 20 recommends a discontinuity loss coefficient of 0.5 for a sharp entrance channel. Reference 21 recommends a value of 2.7 to

properly account for the vena contracta (reduction in cross section) when dealing with near saturated water entering a narrow crack.

The friction factor for turbulent flow (Reynolds number > 4000) is determined from Reference 22.

$$\frac{1}{\sqrt{f}} = -2 \log_{10} \left(\frac{\varepsilon}{3.7 D_H} + \frac{2.52}{Re\sqrt{f}} \right)$$

where:

f = friction factor

ε = surface roughness

D_H = hydraulic diameter

Re = Reynolds number.

For laminar flow between parallel plates, Reference 20 recommends,

$$f = \frac{96}{Re}$$

which occurs below about $R_e = 2000$. In the transition range between $2000 < R_e < 4000$, a best estimate friction factor is determined by interpolating between the friction factor at $R_e = 2000$ and that at $R_e = 4000$.

For the turbulent friction factor equation, and for the transition range, an iterative approach must be taken to solve for the friction factor.

Reference 16 recommends a value of 5 μm (0.000197 inches) for the surface roughness of fatigue cracks. For more tortuous paths, and extremely small crack opening displacements, additional losses might be input with increased values for K. However, this effect will be quite small for crack opening widths which will produce detectable leakage in a power piping system.

For the pipe region filled with subcooled water, the flow can be determined by standard incompressible flow methodology. For saturated steam flow, the mass flow rate versus inlet total pressure may be determined directly from the charts of fL/D from Reference 23. Similarly, Reference 23 provides charts for the blowdown of water and steam-water mixtures. These are incorporated as tables in **pc-LEAK**.

In evaluating the flow of subcooled water, which flashes as the static pressure reaches saturation, a two-step approach is used. For the subcooled portion of the flow, the incompressible flow equation is used:

$$P_{T,inlet} - P_{sat} = (K_{inlet} + 1.0 + \frac{fL}{D_H})\ 1/2\ \rho V^2$$

where:

$P_{T,inlet}$ = pressure inside pipe

P_{sat} = saturation pressure associated with water temperature in pipe

ρ = liquid density

V = velocity

K_{inlet} = inlet plus discontinuity loss coefficient

1.0 = total to static pressure loss coefficient at the downstream end of the flow

From this equation, the length (fL_1/D) of channel to bring fluid from its subcooled condition to a flashing saturated mixture may be determined as a function of mass flux. This is illustrated in Figure 5-1.

In length L_2, a two-phase homogeneous mixture flows and this length may be determined for saturated water from the Reference 22 charts. For small values of fL_2/D, the saturation flashing point may occur just at the exit of the crack, such that the flow can be approximately determined solely based upon flow of liquid water. When the inlet pressure is near saturation pressure, the flow

may be approximately determined from the Reference 22 charts. In between, a combined flow situation exists.

The leakage was calculated for a BWR operating temperature of 550°F and normal operating pressure of 1047 psig for the suction side and 1254 psig for the discharge. Since torsional moments were included in the critical flaw size calculations, the leakage was calculated considering normal operating stresses (without SSE loads) including the torsional moments. The leakage results are presented in Figures 5-2 through 5-4 as a function of crack size for the three locations. Notice that at each location, the leakage is determined separately for the three welds. Table 5-2 shows the predicted leakage at various fractions of the critical flaw size for each case.

5.3 Crack Growth Analysis for Circumferential Through-Wall Flaws

In order to help make decisions relative to the requirements of the leakage detection system at Fermi 2, crack growth analyses were performed to determine the time it takes for an initial through-wall flaw of half the critical flaw size to propagate around the circumference. The analyses were performed using the **pc-CRACK** computer software [15]. The fracture mechanics model selected from **pc-CRACK** library for use in the analyses was a circumferential through-wall crack in a cylindrical shell under tension and bending.

Even though all welds at the affected locations have been treated against IGSCC using NUREG-0313 accepted processes, it was conservatively assumed that crack growth is due to IGSCC. The crack growth law used was obtained from NUREG-0313, Revision 2 [5] and is given by:

$$\frac{da}{dt} = 3.59 \times 10^{-8} K_I^{2161} \text{ inches per hour}$$

where K_I = stress intensity factor ($ksi\sqrt{in}$).

Because the initial flaw is a through-wall flaw, butt weld residual stresses are expected to be relieved, and, therefore, only the sustained piping stresses are considered in the evaluation.

Results of the analyses are presented in Figures 5-7 through 5-9 for the three locations. The results are further summarized in Table 5-3. It can be seen from this table that it takes on the order of months for a crack to grow from one fraction of the critical flaw size to another. In fact, it can be seen that it takes at least one cycle (over eighteen months) for a through-wall crack at half the critical flaw size to grow to three quarters the critical flaw size.

5.4 LBB Evaluation Results and Discussions

As expected, the leakage calculated for the 28-inch suction line is significantly greater than the leakages calculated for the 12-discharge risers at various fractions of the critical flaw size. In fact the leakage for the 28-inch suction line is greater than 1.5 gpm from through-wall flaw sizes as low as one-quarter of the critical flaw size. The most limiting location on the discharge risers are the safe end-to-pipe welds where the leakage could be as low as 0.2 gpm at one-quarter the critical flaw size. However, at half the critical flaw size, the leakage on the discharge lines are all greater than 1.5 gpm. The relatively low leakage at the safe end-to-pipe weld on the discharge risers can be attributed to small critical flaw sizes resulting from the high stresses calculated at these locations. Nevertheless, the leakages presented in Table 5-2 can be compared to the leak detection system of the plant to determine at which fraction of the critical flaw size can be detected. Having determined the detectable leakage, the IGSCC growth evaluation presented in Table 5-3 can be used to determine how long it will take for a through-wall flaw at the detectable leakage size to grow to the critical flaw size. The plant in this way can determine if there is adequate time to take timely action once a leak is detected.

Table 5-1

Summary of Critical Flaw Size

		Total Stress	Tension Stress	Critical flaw size (inch)		
Location	Weld	(ksi)	(ksi)	Tension	Bending	Combined
Loop A N2F	N-SE	8.913	2.883	11.170	14.755	13.595
	SE-P	14.654	4.694	4.950	7.541	6.711
	P-E	11.671	4.694	7.333	10.290	9.101
Loop B N2D	N-SE	8.724	2.883	11.381	15.019	13.817
	SE-P	14.026	4.694	4.644	8.060	6.917
	P-E	9.472	4.694	9.423	12.682	11.067
Loop B N1B	N-SE	7.360	3.548	24.083	31.589	27.971
	SE-P	8.119	3.994	20.926	28.023	24.532
	P-E	7.223	3.994	23.543	30.889	26.827

Table 5-2

LBB Evaluation Results for Detectable Leakage
(Pressure + Resultant Moment Stresses at Leak)

			Leakage at Fraction of Critical Flaw Size (gpm)		
Location	Weld	Critical Flaw Size (in)	One-quarter	One-half	Three-quarters
Loop A N2F	N-SE	13.60	0.58	4.20	13.31
	SE-P	6.71	0.25	1.69	5.22
	P-E	9.10	0.36	2.57	8.12
Loop B N2D	N-SE	13.82	0.51	3.78	12.05
	SE-P	6.92	0.23	1.57	4.87
	P-E	11.07	0.52	3.74	12.30
Loop B N1B	N-SE	27.97	1.74	11.92	40.19
	SE-P	24.53	1.59	10.95	35.22
	P-E	26.83	2.13	14.85	46.99

Table 5-3

Summary of Through-Wall IGSCC Growth Evaluation

Location	Weld	Critical Flaw Size (in)	Time from ½ to ¾ Critical Flaw Size (months)	Time from ¾ to Critical Flaw Size (months)
Loop A N2F	N-SE	13.60	41	19
	SE-P	6.71	21	11
	P-E	9.10	32	15
Loop B N2D	N-SE	13.82	50	23
	SE-P	6.92	25	14
	P-E	11.07	34	15
Loop B N1B	N-SE	27.47	56	25
	SE-P	24.53	46	21
	P-E	26.83	39	18

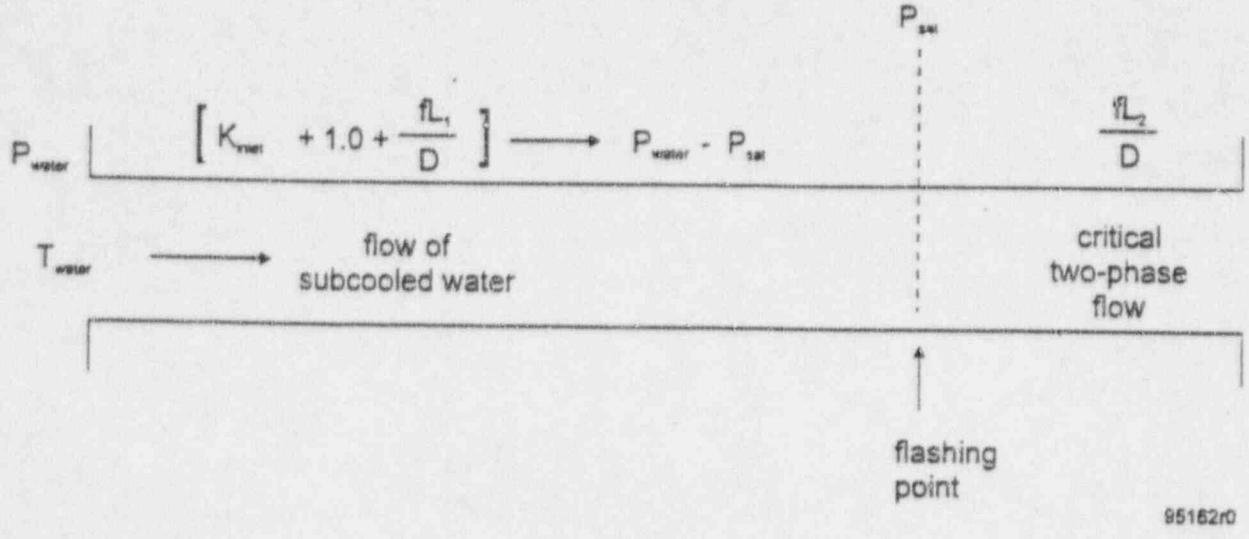

Figure 5-1. Flow of Subcooled Water Through a Crack

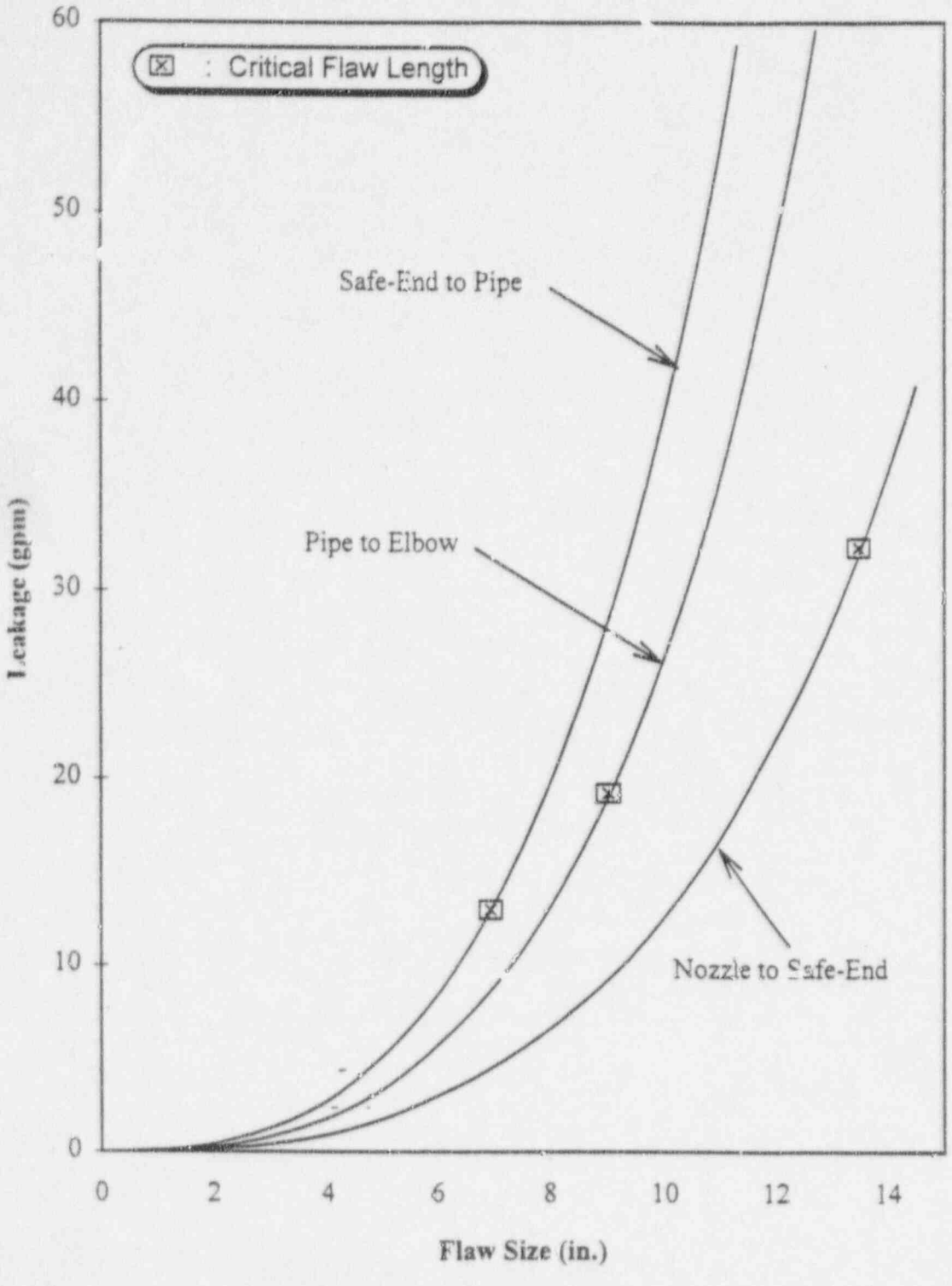

Figure 5-2. Leakage Versus Crack Size for Riser N2F on Loop A

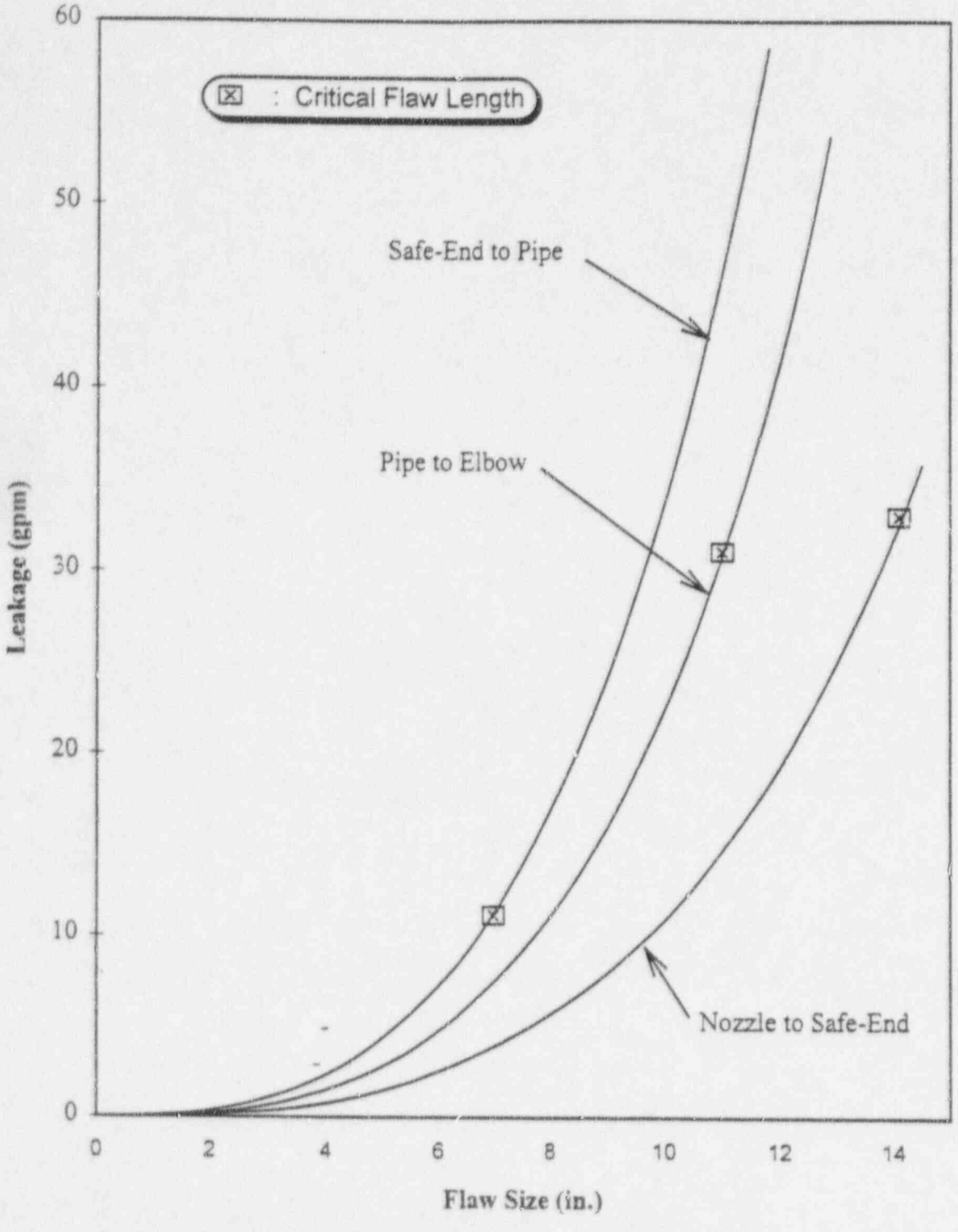

Figure 5-3. Leakage Versus Crack Size for Riser N2D on Loop B

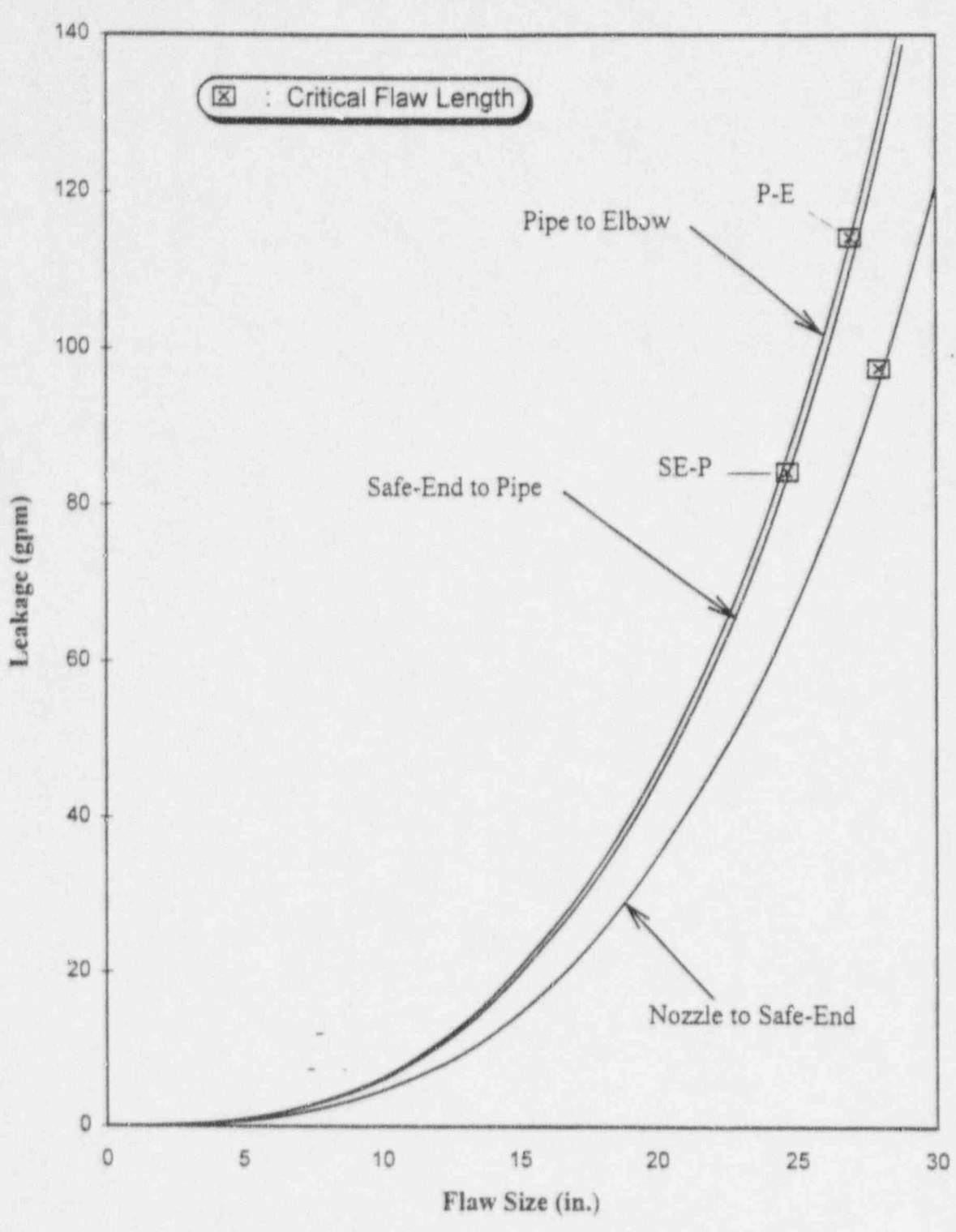

Figure 5-4. Leakage Versus Crack Size for Riser NIB on Loop B

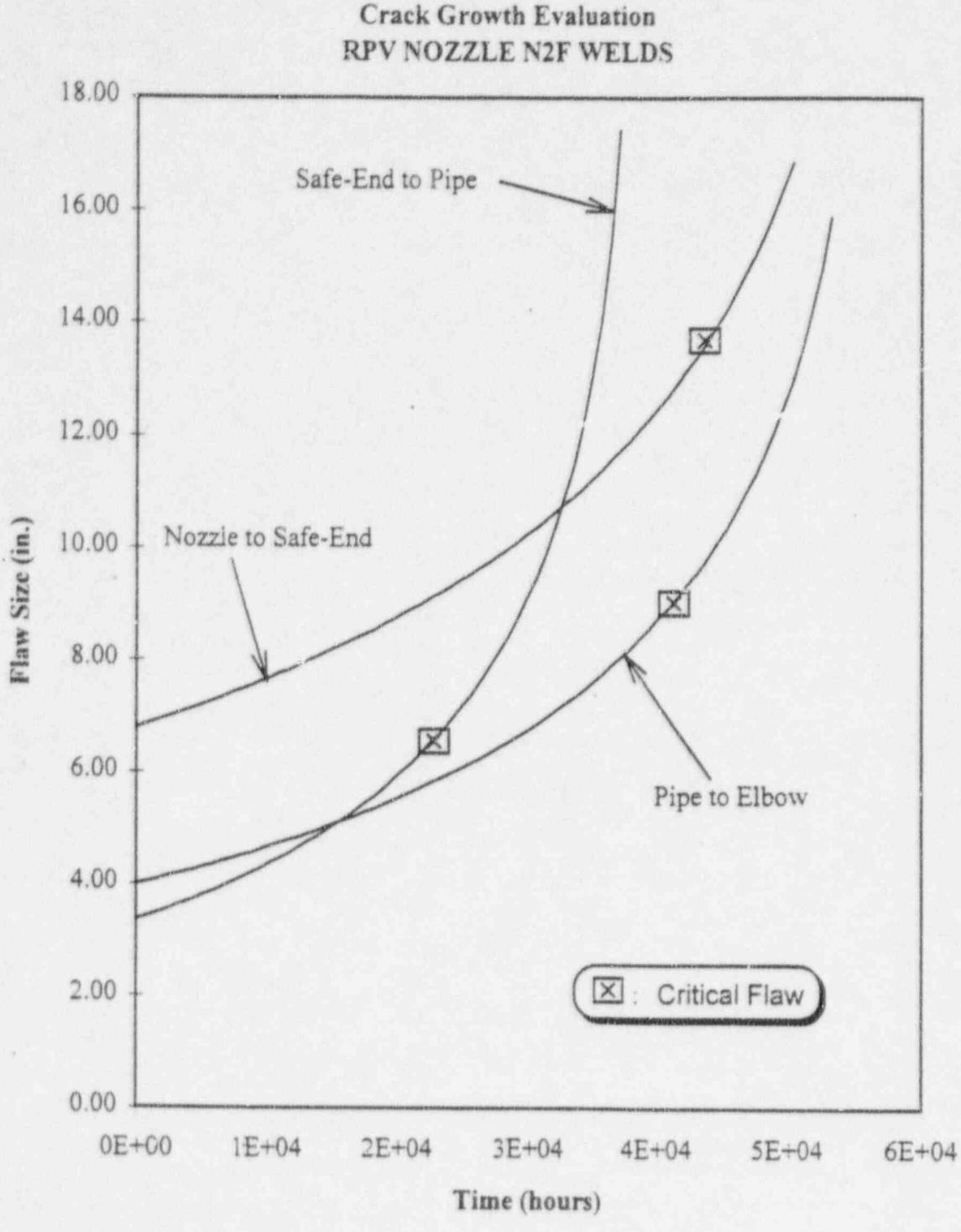

Figure 5-5. Crack Growth Analyses Results for Riser N2F on Loop A

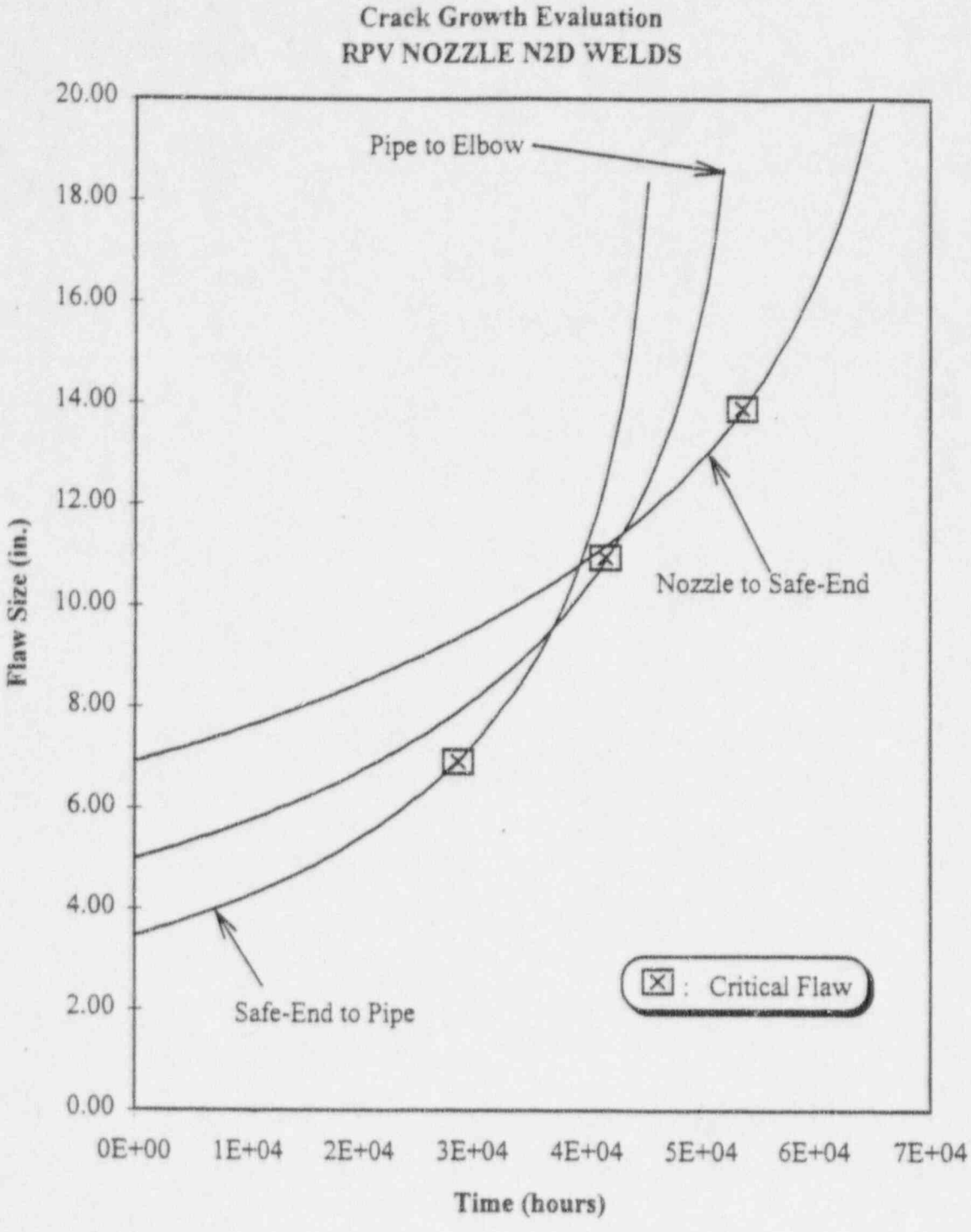

Figure 5-6. Crack Growth Analyses Results for Riser N2D on Loop B

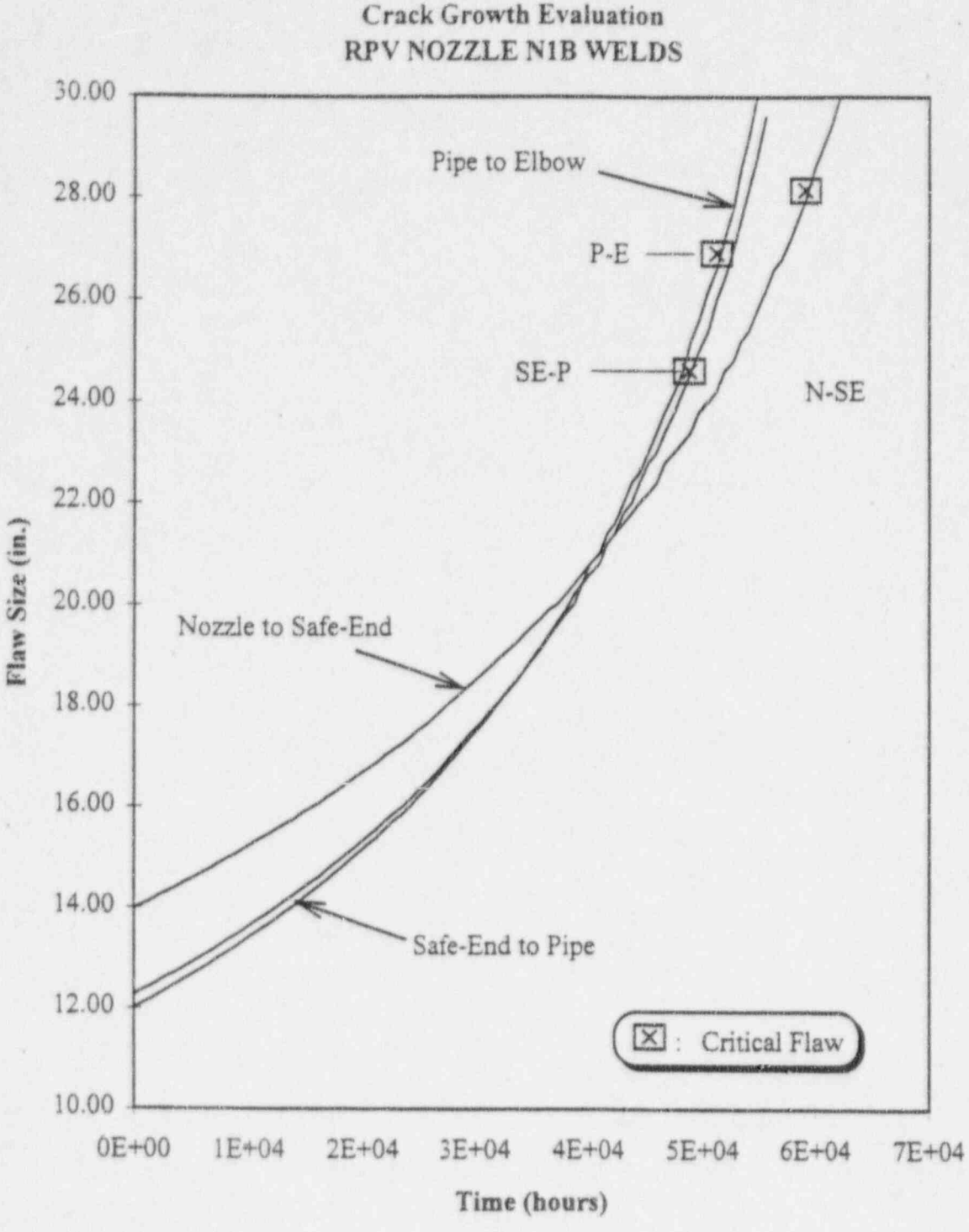

Figure 5-7. Crack Growth Analyses Results for Riser N1B on Loop B

6.0 SUMMARY AND CONCLUSIONS

Leak-before-break (LBB) evaluations are performed for recirculation piping welds at Ferm-2 in accordance with the requirements of NUREG-1061, Volume 3. In the evaluations, circumferential flaws were considered, since they are more limiting. Critical flaw sizes and leakage rates through fractions of the critical flaw sizes were calculated for three welds at each of three locations adjacent to the reactor pressure vessel on discharge risers N2F and N2D as well as suction line N1B (total of nine welds). Times to grow from various sub-critical flaw sizes to critical flaw sizes were also determined.

Based on these evaluations, the following conclusions are provided.

- Predicted leakage rates in the 28-inch suction line are relatively large for all flaw sizes. At one-quarter the critical flaw size, the leakage in this pipe is at least 1.5 gpm. At one-half the critical flaw size, the leakage is at least 10 gpm. The leakage rate is at least 35 gpm at three quarter the critical flaw size in this pipe.

- The safe end-to-pipe weld is the most limiting location on the discharge risers. At one quarter the critical flaw size, the calculated leakage is about 0.2 gpm and increases to 1.5 gpm at one half the critical flaw size. The leakage at this location is approximately 5 gpm at three quarter the critical flaw size. The other weld locations on the two discharge lines have leakage rates of at least 0.3 gpm at one quarter the critical flaw size, 2.5 gpm at one half the critical flaw size and 12 gpm at three quarter the critical flaw size.

- IGSCC evaluation performed using the NUREG-0313, Revision 2 bounding crack growth law showed that it takes at least one cycle (over eighteen months) for a through-wall crack at half the critical flaw size to grow to three quarters the critical flaw size. This demonstrates that there is adequate time for the plant to take appropriate action before the critical flaw size is reached once the leakage rates determined in this report are detected by the plant monitoring systems.

7.0 REFERENCES

1. NUREG-1061, Volume 3, "Report of the U. S. Nuclear Regulatory Commission Piping Review Committee - Evaluation of Potential for Pipe Breaks", prepared by the Piping Review Committee, NRC, April 1985.

2. EPRI Report NP-4991, "Application of the Leak-Before-Break Approach to BWR Piping" December 1986.

3. NUREG-1061, Volume 4, "Report of the U.S. Nuclear Regulatory Commission on Piping Review Committee - Evaluation of Other Dynamic Loads and Load Combinations", prepared by the Piping Review Committee, NRC, April 1985.

4. NUREG-0927, Revision 1, "Evaluation of Water Hammer Occurrences in Nuclear Power Plants, Technical Finding Relevant to USI A-1", March 1984.

5. Hazelton, W. S. and Koo, W.H., "Technical Report on Material Selection and Processing Guidelines for BWR Coolant Pressure Boundary Piping", NUREG-0313, Rev. 2, USNRC, January 1988.

6. ASME Section XI Task Group for Piping Flaw Evaluation, "Evaluation of Flaws in Austenitic Steel Piping", Journal of Pressure Vessel Technology, Volume 108, August 1986.

7. "Evaluation and Discussion of EPRI's High Energy Pipe Rupture Experiments", EPRI Report No. NP-5531, by Structural Integrity Associates and S. Levy, Inc., SI Report No. SIR-86-034, September, 1987.

8. ASME Boiler and Pressure Vessel Code, Section III Appendices and Section II, Part A, 1989 Edition.

9. Detroit Edison Calculation and Drawings (SI File Nos. DECO-01Q-201 and DECO-01Q-203).
   DC-2674 Vol. V DCD-RPS Loop 'A'
   DC-2675 Vol. III DCD-RPS Loop 'B'
   M-5356-5 Rev. 0 - ISI Drawing for Loop 'A'
   M-5358-5 Rev. 0 - ISI Drawing for Loop 'B'
   M-5359-5 Rev. B - ISI Drawing for Loop 'A'

10. Combustion Engineering Drawings (SI File No. DECO-01Q-202).
    232 908 Rev. 3 (DECO File No. R1-90)
    232 897 Rev. 3 (DECO File No. R1-132)

11. General Electric Drawings/Specification (SI File No. DECO-01Q-202 and DECO-01Q-204).
117C4384, Rev. 2 & 117C4384AB, Rev. 3 (DECO File # R1-294)
761E214 Page 1 Rev. 11, Page 2 Rev. 10 & Page 3 Rev. 7 (DECO File # R1-174)
21A9318 Rev. 3 & 21A9318AB Rev. 1 (DECO File R1-198)

12. Kumar, V., et al., "An Engineering Approach for Elastic-Plastic Fracture Analysis," EPRI NP-1931, July 1981.

13. Kumar, V., et al., "Advances in Elastic-Plastic Fracture Analysis", EPRI NP-3607, August 1984.

14. Kumar, V., et al., "Elastic Plastic Fracture Analysis of Through-wall and Surface Flaws in Cylinders," EPRI NP-5596, January 1988.

15. Structural Integrity Associates, Inc., "**pc-CRACK** Fracture Mechanics Software", Version 2.1, User's Manual, May 1992.

16. "**pc-LEAK** Calculation of Leakage Rates From Through-Wall Cracks", Version 1.0, Structural Integrity Associates, August 1990.

17. Paris, P.C., and Tada, H. , "The Application of Fracture Proof Design Methods Using Tearing Instability Theory to Nuclear Piping Postulating Circumferential Through-Wall Cracks", NUREG/CR-3464, September 1983.

18. Klecker, R., Brust, F., and Wilkowski, G., "NRC Leak-Before-Break (LBB.NRC) Analysis Method for Circumferentially Through-Wall Cracked Pipes Under Axial Plus Bending Loads", NUREG/CR-4572, BMI-2134, May 1986.

19. Rohsenow and Choi, "Heat, Mass, and Momentum Transfer", Prentice-Hall, New Jersey, 1961.

20. Blevins, R. D., "Applied Fluids Dynamics Handbook", Van Nostrand Reinhold Co., New York, 1984.

21. "Calculation of Leak Rates Through Cracks in Pipes and Tubes", EPRI Report NP-3395, Electric Power Research Institute, December 1983.

22. Marks Standard Handbook for Mechanical Engineers, Eighth Edition, McGraw Hill, New York, 1978.

23. Lahey, R. J., and Moody, F. J., "Thermal Hydraulics of Boiling Water Reactors", American Nuclear Society, 1977.

APPENDIX A

Loads and Stresses

DECO-01Q, FERMI NUCLEAR PLANT Unit 2

RECIRCULATION SYSTEM - RV NOZZLE N2F (INLET)

Nozzle to Safe-End Weld- LOOP A

NODE NO. 378

OD (IN):	14.375
T (IN):	1.1875
ID (IN):	12
P (KSI):	1.254
A (IN^2):	49.198
Z (IN^3):	150.007

Moment Arm 4.0

	FORCES AND MOMENTS							TOTAL	AXIAL
LOAD	FA (KIPS)	FB (KIPS)	FC (KIPS)	Faxial (KIPS)	MA (IN-KIPS)	MB (IN-KIPS)	MC (IN-KIPS)	MOMENT (IN-KIPS)	STRESS (KSI)
P	-----	-----	-----		-----	-----	-----	-----	2.883
THERMAL1	1.1	-8.5	-3.9	1.10	199.3	-144.9	391.2	462	3.104
THERMAL2	1.5	-3	-1	1.50	48.7	-4.5	181.7	188	1.285
THERMAL3	1.3	-5.8	-3.2	1.30	157.6	-115.7	289.7	350	2.356
DW	0	1.3	-0.2	0.00	8.4	-10.4	-49.0	51	0.339
SSEI 1	3.2	3.1	3.8	3.20	185.2	217.3	114.1	307	2.115
SSEI 2	0.6	1.4	0.5	0.60	27.1	31.6	54.6	69	0.470
SSEI 3	1.8	3.2	2.6	1.80	132.9	138.1	103.0	218	1.487
SSED 1	-0.1	0.2	0.1	-0.10	-5.5	5.6	-12.2	15	0.099
SSED 3	0	-0.2	-0.1	0.00	5.1	-3.5	7.0	9	0.062
SSED 6	0	-0.7	-0.2	0.00	13.6	-8.0	23.9	29	0.191
Max. SSED 3&6	0	-0.7	-0.2	0.00	13.6	-8	23.9	29	0.191
SSE X									2.117
SSE Y									0.470
SSE Z									1.499
SSE_XY									2.587
SSE_YZ									1.969
THERMAL									3.104
SEISMIC									2.587

DECO-01Q, FERMI NUCLEAR PLANT Unit 2

RECIRCULATION SYSTEM - RV NOZZLE N2F (INLET)

Safe-End TO Pipe Weld- LOOP A

NODE NO. 378

OD (IN):	12.875
T (IN):	0.71875
ID (IN):	11.4375
P (KSI):	1.254
A (IN^2):	27.449
Z (IN^3):	79.038

Moment Arm 4.0

LOAD	FORCES AND MOMENTS							TOTAL MOMENT (IN-KIPS)	AXIAL STRESS (KSI)
	FA (KIPS)	FB (KIPS)	FC (KIPS)	Faxial (KIPS)	MA (IN-KIPS)	MB (IN-KIPS)	MC (IN-KIPS)		
P	-----	-----	-----		-----	-----	-----	-----	4.694
THERMAL1	1.1	-8.5	-3.9	1.10	199.3	-113.7	323.2	396	5.055
THERMAL2	1.5	-3	-1	1.50	48.7	3.5	157.7	165	2.143
THERMAL3	1.3	-5.8	-3.2	1.30	157.6	-90.1	243.3	304	3.888
DW	0	1.3	-0.2	0.00	8.4	-8.8	-38.6	40	0.512
SSEI 1	3.2	3.1	3.8	3.20	185.2	186.9	89.3	278	3.632
SSEI 2	0.6	1.4	0.5	0.60	27.1	27.6	43.4	58	0.757
SSEI 3	1.8	3.2	2.6	1.80	132.9	117.3	77.4	193	2.513
SSED 1	-0.1	0.2	0.1	-0.10	-5.5	4.8	-10.6	13	0.166
SSED 3	0	-0.2	-0.1	0.00	5.1	-2.7	5.4	8	0.100
SSED 6	0	-0.7	-0.2	0.00	13.6	-6.4	18.3	24	0.300
Max. SSED 3&6	0	-0.7	-0.2	0.00	13.6	-6.4	18.3	24	0.300
SSE X									3.636
SSE Y									0.757
SSE Z									2.531
SSE_XY									4.393
SSE_YZ									3.288
THERMAL									5.055
SEISMIC									4.393

DECO-01Q, FERMI NUCLEAR PLANT Unit 2

RECIRCULATION SYSTEM - RV NOZZLE N2F (INLET)

Pipe to Elbow Weld- LOOP A

NODE NO. 376

OD (IN): 12.875
T (IN): 0.71875
ID (IN): 11.4375
P (KSI): 1.254
A (IN^2): 27.449
Z (IN^3): 79.038

LOAD	FORCES AND MOMENTS							TOTAL MOMENT (IN-KIPS)	AXIAL STRESS (KSI)
	FA (KIPS)	FB (KIPS)	FC (KIPS)	Faxial (KIPS)	MA (IN-KIPS)	MB (IN-KIPS)	MC (IN-KIPS)		
P	----	----	----		----	----	----	----	4.694
THERMAL1	1.1	8.5	3.9	1.10	199.3	14.1	-107.2	227	2.909
THERMAL2	1.5	3	1	1.50	48.7	-27.7	-81	98	1.301
THERMAL3	1.3	5.8	3.2	1.30	157.6	9.8	-97.6	186	2.396
DW	0	-0.9	0.2	0.00	8.4	3	10.4	14	0.173
SSEI 1	3.2	3.1	3.8	3.20	185.2	91	81.2	222	2.922
SSEI 2	0.6	1.4	0.5	0.60	27.1	17.3	10.7	34	0.451
SSEI 3	1.8	3.2	2.5	1.80	132.9	58.7	41.1	151	1.976
SSED 1	-0.1	-0.2	-0.1	-0.10	-5.5	-1.6	143.7	144	1.823
SSED 3	0	0.2	0.1	0.00	5.1	0.6	26.7	27	0.344
SSED 6	0	0.7	0.2	0.00	13.6	0.5	76.6	78	0.984
Max. SSED 3&6	0	0.7	0.2	0.00	13.6	0.6	76.6	78	0.984
SSE X									3.444
SSE Y									0.451
SSE Z									2.208
SSE_XY									3.895
SSE_YZ									2.658
THERMAL									2.909
SEISMIC									3.895

DECO-01Q, FERMI NUCLEAR PLANT Unit 2

RECIRCULATION SYSTEM - RV NOZZLE N2D (INLET)

Nozzle to Safe-End Weld- LOOP B

NODE NO. 318

OD (IN):	14.375
T (IN):	1.1875
ID (IN):	12
P (KSI):	1.254
A (IN^2):	49.198
Z (IN^3):	150.007

Moment Arm 4.0

	FORCES AND MOMENTS							TOTAL	AXIAL
LOAD	FA (KIPS)	FB (KIPS)	FC (KIPS)	Faxial (KIPS)	MA (IN-KIPS)	MB (IN-KIPS)	MC (IN-KIPS)	MOMENT (IN-KIPS)	STRESS (KSI)
P	-----	-----	-----		-----	-----	-----	-----	**2.883**
THERMAL1	-0.4	6.1	-0.1	-0.40	7	6.5	-364.6	365	**2.440**
THERMAL2	0.4	4.7	-2.4	0.40	113.5	-113.9	-243.6	292	1.954
THERMAL3	0	4	0.1	0.00	-3	10.2	-235.7	236	1.573
DW	0.1	1.5	0.1	0.10	-5.5	0.8	-53.3	54	**0.359**
SSEI 1	1.3	2.7	2.3	1.30	96.1	139.3	171.8	241	1.634
SSEI 2	0.6	4.3	0.6	0.60	24.9	25.5	178.2	182	1.224
SSEI 3	2.3	5.4	1.1	2.30	5.1	62.8	251.3	265	1.812
SSED 1	0	0.3	-0.2	0.00	7.8	-7.3	-12.7	17	0.111
SSED 3	0	-0.1	-0.1	0.00	2.9	-2.4	8.0	9	0.059
SSED 6	0.1	-0.3	-0.1	0.10	8	-4.1	20.7	22	0.152
Max. SSED 3&6	0.1	-0.3	-0.1	0.10		-4.1	20.7	22	0.152
SSE X									1.638
SSE Y									1.224
SSE Z									1.819
SSE_XY									2.861
SSE_YZ									3.042
THERMAL									2.440
SEISMIC									3.042

DECO-01Q, FERMI NUCLEAR PLANT Unit 2

RECIRCULATION SYSTEM - RV NOZZLE N2D (INLET)

Safe-End to Pipe Weld- LOOP B

NODE NO. 318

OD (IN):	12.875
T (IN):	0.71875
ID (IN):	11.4375
P (KSI):	1.254
A (IN^2):	27.449
Z (IN^3):	79.038

Moment Arm 4.0

LOAD	FORCES AND MOMENTS							TOTAL MOMENT (IN-KIPS)	AXIAL STRESS (KSI)
	FA (KIPS)	FB (KIPS)	FC (KIPS)	Faxial (KIPS)	MA (IN-KIPS)	MB (IN-KIPS)	MC (IN-KIPS)		
P	-----	-----	-----		-----	-----	-----	-----	4.694
THERMAL1	-0.4	6.1	-0.1	-0.40	7	5.7	-315.8	316	4.012
THERMAL2	0.4	4.7	-2.4	0.40	113.5	-94.7	-206.0	254	3.222
THERMAL3	0	4	[illegible]	0.00	-3	9.4	-203.7	204	2.580
DW	0.1	1.5	0.1	0.10	-5.5	0.0	-41.3	42	0.531
SSEI 1	1.3	2.[illegible]	2.3	1.30	96.1	120.9	150.2	215	2.773
SSEI 2	0.6	4.[illegible]	0.6	0.60	24.9	20.7	143.8	147	1.887
SSEI 3	2.3	5.4	1.1	2.30	55.1	54.0	208.1	222	2.892
SSED 1	0	0.3	-0.2	0.00	7.8	-5.7	-10.3	14	0.179
SSED 3	0	-0.1	-0.1	0.00	2.9	-1.6	7.2	8	0.100
SSED 6	0.1	-0.3	-0.1	0.10	7.8	-3.3	18.3	20	0.259
Max. SSED 3&6	0.1	-0.3	-0.1	0.10	7.8	-3.3	18.3	20	0.259
SSE X									2.779
SSE Y									1.887
SSE Z									2.903
SSE_XY									4.666
SSE_YZ									4.790
THERMAL									4.012
SEISMIC									4.790

DECO-01Q, FERMI NUCLEAR PLANT Unit 2

RECIRCULATION SYSTEM - RV NOZZLE N2D (INLET)

Pipe to Elbow Weld- LOOP B

NODE NO. 316

OD (IN):	12.875
T (IN):	0.71875
ID (IN):	11.4375
P (KSI):	1.254
A (IN^2):	27.449
Z (IN^3):	79.038

	FORCES AND MOMENTS							TOTAL	AXIAL
LOAD	FA (KIPS)	FB (KIPS)	FC (KIPS)	Faxial (KIPS)	MA (IN-KIPS)	MB (IN-KIPS)	MC (IN-KIPS)	MOMENT (IN-KIPS)	STRESS (KSI)
P	-----	-----	-----		-----	-----	-----	-----	4.694
THERMAL1	-0.4	-6.1	0.1	-0.40	7	-9.4	161.6	162	2.065
THERMAL2	0.4	-4.7	2.4	0.40	113.5	33.1	85.3	146	1.859
THERMAL3	0	-4	-0.1	0.00	-3	-7.6	100.9	101	1.281
DW	0.1	-1.1	-0.1	0.10	-5.5	1.2	3.8	10	0.136
SSEI 1	1.3	2.7	2.2	1.30	96.1	70.7	91	150	1.946
SSEI 2	0.6	4.3	0.6	0.60	24.9	9.3	39.9	48	0.628
SSEI 3	2.3	5.4	1.1	2.30	55.1	42.2	111.1	131	1.741
SSED 1	0	-0.3	0.2	0.00	7.8	1.7	4	9	0.113
SSED 3	0	0.1	0.1	0.00	2.9	0.3	-4.2	5	0.065
SSED 6	0.1	0.3	0.1	0.10	7.8	-0.5	-10.8	13	0.172
Max. SSED 3&6	0.1	0.3	0.1	0.10	7.8	-0.5	-10.8	13	0.172
SSE X									1.949
SSE Y									0.628
SSE Z									1.750
SSE_XY									2.578
SSE_YZ									2.378
THERMAL									2.065
SEISMIC									2.578

DECO-01Q, FERMI NUCLEAR PLANT Unit 2

RECIRCULATION SYSTEM - RV NOZZLE N1B (OUTLET)

Nozzle to Safe-End Weld- LOOP B

NODE NO. 001

OD (IN):	29.375
T (IN):	1.78125
ID (IN):	25.8125
P (KSI):	1.047
A (IN^2):	154.414
Z (IN^3):	1004.79

Moment Arm 4.5

	FORCES AND MOMENTS							TOTAL	AXIAL
LOAD	FA (KIPS)	FB (KIPS)	FC (KIPS)	Faxial (KIPS)	MA (IN-KIPS)	MB (IN-KIPS)	MC (IN-KIPS)	MOMENT (IN-KIPS)	STRESS (KSI)
P	-----	-----	-----		-----	-----	-----	-----	**3.548**
THERMAL1	-5.3	14.7	3.5	-5.30	-1239.8	-342.5	-323.8	1326	1.354
THERMAL2	-6	8.2	0.3	-6.00	-584	-111.4	-561.4	818	0.853
THERMAL3	-3.6	10.4	2.6	-3.60	-892.4	-261.7	-235.3	959	0.978
DW	-0.1	-0.4	-0.2	-0.10	-21.9	24.4	96.2	102	**0.102**
SSEI 1	3.1	11	3.8	3.10	265.1	226.9	667.0	753	0.769
SSEI 2	2.5	16.6	2.1	2.50	103.7	167.5	1056.4	1075	1.086
SSEI 3	3.2	19	3.9	3.20	182.1	246.9	1210.0	1248	1.263
SSED 1	-0.2	0	0	-0.20	-2.1	-1.5	-29.2	29	0.030
SSED 3	0	-0.1	-0.2	0.00	33.8	12.9	-7.1	37	0.037
SSED 6	0.1	-0.8	-0.8	0.10	114.5	46.6	-48.2	133	0.133
Max. SSED 3&6	0.1	-0.8	-0.8	0.10	114.5	46.625	-48.225	133	0.133
SSE X									0.770
SSE Y									1.086
SSE Z									1.270
SSE_XY									1.856
SSE_YZ									2.356
THERMAL									1.354
SEISMIC									2.356

DECO-01Q, FERMI NUCLEAR PLANT Unit 2

RECIRCULATION SYSTEM - RV NOZZLE N1B (OUTLET)

Safe-End to Pipe Weld- LOOP B

NODE NO. 001

OD (IN):	28.4375
T (IN):	1.5625
ID (IN):	25.3125
P (KSI):	1.047
A (IN^2):	131.922
Z (IN^3):	840.484

Moment Arm 4.5

LOAD	FORCES AND MOMENTS							TOTAL MOMENT (IN-KIPS)	AXIAL STRESS (KSI)
	FA (KIPS)	FB (KIPS)	FC (KIPS)	Faxial (KIPS)	MA (IN-KIPS)	MB (IN-KIPS)	MC (IN-KIPS)		
P	-----	-----	-----		-----	-----	-----	-----	3.994
THERMAL1	-5.3	14.7	3.5	-5.30	-1239.8	-310.7	-190.6	1292	1.578
THERMAL2	-6	8.2	0.3	-6.00	-584	-108.6	-487.0	768	0.959
THERMAL3	-3.6	10.4	2.6	-3.60	-892.4	-238.1	-141.1	934	1.139
DW	-0.1	-0.4	-0.2	-0.10	-21.9	22.6	92.6	98	0.117
SSEI 1	3.1	11	3.8	3.10	265.1	192.5	567.4	655	0.803
SSEI 2	2.5	16.6	2.1	2.50	103.7	148.5	906.0	924	1.118
SSEI 3	3.2	19	3.9	3.20	182.1	211.5	1037.8	1075	1.303
SSED 1	-0.2	0	0	-0.20	-2.1	-1.5	-29.2	29	0.036
SSED 3	0	-0.1	-0.2	0.00	33.8	11.1	-6.1	36	0.043
SSED 6	0.1	-0.8	-0.8	0.10	114.5	39.4	-41.0	128	0.153
Max. SSED 3&6	0.1	-0.8	-0.8	0.10	114.5	39.375	-40.975	128	0.153
SSE X									0.804
SSE Y									1.118
SSE Z									1.312
SSE_XY									1.922
SSE_YZ									2.430
THERMAL									1.578
SEISMIC									2.430

DECO-01Q, FERMI NUCLEAR PLANT Unit 2

RECIRCULATION SYSTEM - RV NOZZLE N1B (OUTET)

Pipe to Elbow Weld- LOOP B

NODE NO. 003

OD (IN): 28.4375
T (IN): 1.5625
ID (IN): 25.3125
P (KSI): 1.047
A (IN^2): 131.922
Z (IN^3): 840.484

LOAD	FORCES AND MOMENTS							TOTAL MOMENT (IN-KIPS)	AXIAL STRESS (KSI)
	FA (KIPS)	FB (KIPS)	FC (KIPS)	Faxial (KIPS)	MA (IN-KIPS)	MB (IN-KIPS)	MC (IN-KIPS)		
P	----	----	----		----	----	----	----	3.994
THERMAL1	-5.3	-14.7	-3.5	-5.30	-1239.8	220	704.4	1443	1.757
THERMAL2	-6	-8.2	-0.3	-6.00	-584	100.8	773.7	975	1.205
THERMAL3	-3.6	-10.4	-2.6	-3.60	-892.4	170.2	505.8	1040	1.264
DW	-0.1	-1.1	0.2	-0.10	-21.9	-17	-83.6	88	0.106
SSEI 1	2.9	10.9	3.8	2.90	265.1	228.9	293.9	457	0.566
SSEI 2	2.5	16.5	2	2.50	103.7	113	480.7	505	0.619
SSEI 3	3.2	19	3.7	3.20	182.1	147.9	548.2	596	0.734
SSED 1	-0.2	0	0	-0.20	-2.1	0.5	27.7	28	0.035
SSED 3	0	0.1	0.2	0.00	33.8	-5.2	2.2	34	0.041
SSED 6	0.1	0.8	0.8	0.10	114.5	-19.5	18.8	118	0.141
Max. SSED 3&6	0.1	0.8	0.8	0.10	114.5	-19.5	18.8	118	0.141
SSE X									0.567
SSE Y									0.619
SSE Z									0.747
SSE_XY									1.186
SSE_YZ									1.366
THERMAL									1.757
SEISMIC									1.366

DECO-01Q, FERMI NUCLEAR PLANT Unit 2

RECIRCULATION SYSTEM - RV NOZZLES N2F, N2D and N1B

SUSTAINED STRESSES

Location	Weld	STRESS (ksi)					
		PRESSURE	DEAD WT.	THERMAL	S.S.E.	P+DW+TH	P+DW+TH+SSE
Loop A N2F	N-SE	2.883	0.339	3.104	2.587	6.326	8.913
	SE-P	4.694	0.512	5.055	4.393	10.261	14.654
	P-E	4.694	0.173	2.909	3.895	7.776	11.671
Loop B N2D	N-SE	2.883	0.359	2.440	3.042	5.682	8.724
	SE-P	4.694	0.531	4.012	4.790	9.236	14.026
	P-E	4.694	0.136	2.065	2.578	6.894	9.472
Loop B N1B	N-SE	3.548	0.102	1.354	2.356	5.004	7.360
	SE-P	3.994	0.117	1.578	2.430	5.689	8.119
	P-E	3.994	0.106	1.757	1.366	5.856	7.223